

GHGT-12

Spatial-temporal water column monitoring using multiple, low-cost GasPro-pCO<sub>2</sub> sensors: implications for monitoring, modelling, and potential impact.

S. E. Beaubien<sup>a\*</sup>, S. Graziani<sup>a</sup>, A. Annunziatellis<sup>a,b</sup>, S. Bigi<sup>a</sup>, L. Ruggiero<sup>a</sup>, M. C. Tartarello<sup>a</sup>, S. Lombardi<sup>a</sup>

<sup>a</sup>*Dipartimento di Scienze della Terra, Università di Roma "La Sapienza", P.le Aldo Moro 5, 00185 Rome, Italy*

<sup>b</sup>*ISPRA, Via Vitaliano Brancati 48, 00144 Rome, Italy*

---

**Abstract**

Monitoring of the water column in the vicinity of offshore Carbon Capture and Storage (CCS) sites is needed to ensure site integrity and to protect the surrounding marine ecosystem. In this regard, the use of continuous, autonomous systems is considered greatly advantageous due to the costs and limitations of periodic, ship-based sampling campaigns. While various geochemical monitoring tools have been developed their elevated costs and complexities mean that typically only one unit can be deployed at a time, yielding single point temporal data but no spatial data. To address this the authors have developed low-cost pCO<sub>2</sub> sensors (GasPro-pCO<sub>2</sub>) that are small, robust, stable, and which have a low power consumption, characteristics which allow for the deployment of numerous units to monitor the spatial-temporal distribution of pCO<sub>2</sub>, temperature, and water pressure in surface water environments. The present article details the results of three field deployments at the natural, CO<sub>2</sub>-leaking site near Panarea, Island. While the first consisted of 6 probes placed on the sea floor for a 2.5 month period, the other two involved the deployment of 20 GasPro units along a transect through the water column in the vicinity of active CO<sub>2</sub> seeps over 2 – 4 days. Results show both transport and mixing processes and highlight the dynamic nature of the leakage-induced marine geochemical anomalies. Implications for monitoring programs as well as potential impacts are discussed.

© 2014 The Authors. Published by Elsevier Ltd. This is an open access article under the CC BY-NC-ND license (<http://creativecommons.org/licenses/by-nc-nd/3.0/>).

Peer-review under responsibility of the Organizing Committee of GHGT-12

*Keywords:* offshore CCS; pCO<sub>2</sub>; spatial-temporal monitoring; Panarea

---

---

\* Corresponding author. Tel.: +39-(0)6-49914918; fax: +39-(0)6-49914918.  
*E-mail address:* stanley.beaubien@uniroma1.it

## 1. Introduction

The dynamic nature of marine physical and biochemical processes, combined with the logistical difficulties and high costs of intermittent, manual, ship-based sampling, has led to recent development of continuous and autonomous chemical monitoring tools. In particular, numerous such instruments have been developed for the study of carbonate system parameters [1-3], including  $p\text{CO}_2$ , due to their importance in natural marine processes and for the monitoring of off-shore  $\text{CO}_2$  capture and storage (CCS) sites. Although these instruments are very precise and respond rapidly, they are typically large and costly, meaning that temporal monitoring is usually only conducted at a single point. While providing critical data, such deployments cannot be used to understand processes that affect spatial distributions and movements, such as mixing and transport.

To address this we have developed small, low-power-consuming, and low-cost  $p\text{CO}_2$  gas probes (“GasPro”), which use an NDIR sensor located in a small chamber behind a gas permeable membrane [4,5]. The goal of this development has always been to minimize costs so that multiple units can be deployed simultaneously, thus providing both temporal and spatial data. Here we report the results obtained during three different, multiple-unit GasPro deployments near the natural  $\text{CO}_2$  leakage areas off the coast of Panarea Island, Italy (Fig. 1) and discuss the implications for CCS leakage monitoring and modelling, as well as potential impacts.

## 2. Experimental

### 2.1. GasPro Sensors

Each GasPro unit is housed in a 200 mm long, 78 mm diameter Plexiglas cylinder, weighs 0.7 kg in air, and consumes less than 40 mA during the 2 minute warm-up/analysis period. These sensors can be cabled to a central control unit for real-time control and data transfer or used as stand-alone units with internal batteries and a datalogger. Measurement is based on equilibration of a small-volume headspace, containing a miniature non-dispersive infrared (NDIR) detector, with the surrounding water via diffusion through a gas permeable membrane; equilibration is completely passive and no pumps are used to minimize power consumption. A larger chamber, physically isolated and located behind the sensor chamber, contains control electronics, memory, and batteries. All probes are equipped with an external water temperature sensor, while a pressure sensor was mounted on one probe to monitor tidal fluctuations during two of the three deployments. The GasPro is programmed to make measurements at pre-determined time intervals depending on the study needs and deployment period. When the datalogger unit is used, battery life is on the order of 1 month for a lamp warm-up time of 2 minutes and a sampling frequency of once every 10 minutes and memory is essentially non-limiting with a 2Gb SD card. A more detailed description of the units and their measurement characteristics (e.g. response time, stability, temperature effect) is given in [5].

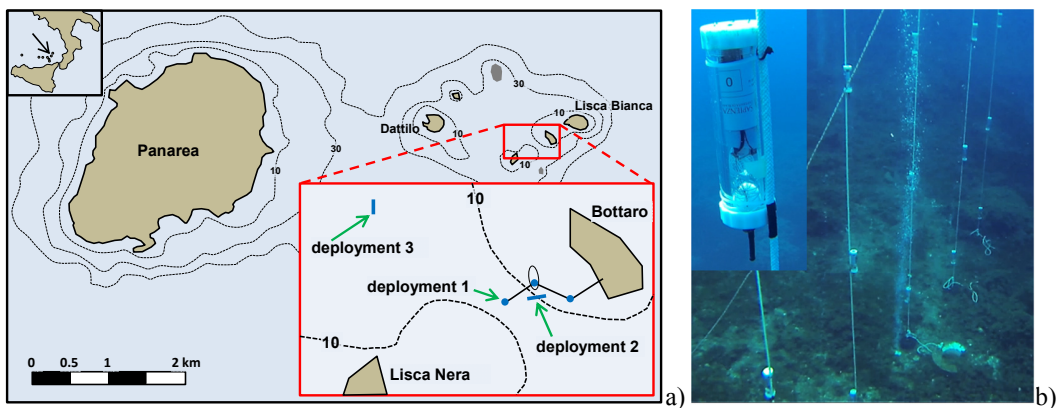


Fig. 1. (a) Map showing Panarea Island and the three deployment locations; (b) photographs of the third GasPro deployment around a central  $\text{CO}_2$  seepage point and a single sensor (insert).

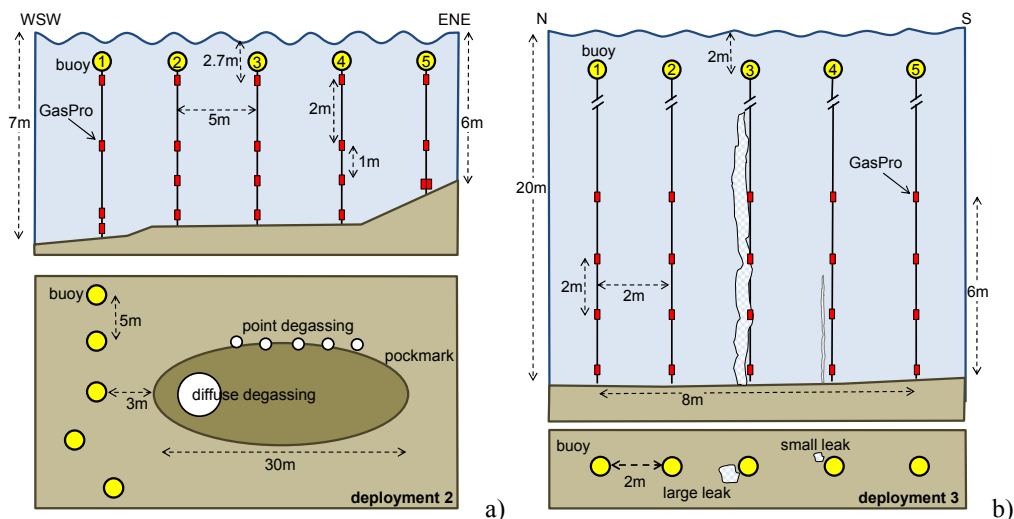


Fig. 2. Schematic drawings of the second GasPro deployment showing: (a) the probes in the water column and (b) their distribution relative to a near-by pockmark with CO<sub>2</sub> seeps. Schematic drawings of the third GasPro deployment showing: (c) the probes in the water column relative to a central gas leakage point on line 3 and a small one on line 4, and (d) a plan-view map of the same.

## 2.2. Deployments

The first deployment, conducted in the summer of 2011 over a 2.5 month period within the EC-funded RISCS project, consisted of two probes positioned 6 m apart on the sea floor in three different areas (located about 50 m apart) that have no, moderate, and high leakage rates (Fig. 1). The 6 probes were connected via an underwater cable to an on-land control station that received pCO<sub>2</sub> and temperature measurements from the probes every 2 hours and transmitted them in real time via GPRS signal to a web-based server. The goal of this monitoring experiment was to test the long-term capabilities of the GasPro in different leakage regimes. As the 3 monitored sites are distant one from the other, this is temporal-only monitoring.

The second deployment, conducted in the summer of 2014 over a 5 day period within the EC-funded ECO<sub>2</sub> project, consisted of the simultaneous deployment of 19 datalogger GasPro units along a 20 m long and 4 m high, vertical water-column transect in 7 m deep water (Fig. 2a). The transect was placed perpendicular to the main current direction and to the long-axis of a near-by CO<sub>2</sub> leaking pockmark (the high leaking site in the first deployment). The temperature and pCO<sub>2</sub> data from all 19 probes (and pressure data from one probe) were recorded once every 10 minutes. The goal of this work was to better understand the temporal results from the first deployment by conducting a 2D monitoring of the water column just outside the pockmark.

The third deployment, conducted in the summer of 2014 over a 2.5 day period within the EC-funded ECO<sub>2</sub> project, consisted of the simultaneous deployment of 20 datalogger GasPro units along an 8 m long and 6 m high, vertical water-column transect in 20 m deep water (Fig. 2b). The transect was positioned parallel to the main current direction with the central vertical line located within a strong single bubble flare. The goal of this transect was to monitor the near-field spatial-temporal distribution of pCO<sub>2</sub> around the flare. As in the previous, the temperature and pCO<sub>2</sub> data from all 20 probes (and pressure data from one probe) were recorded once every 10 minutes.

## 3. Results and Discussion

### 3.1. Deployment 1

Data collected during the entire first deployment is given in Fig. 3a. As trends and values are very similar for the various temperature and CO<sub>2</sub> sensors, a single, representative dataset was chosen for each site.

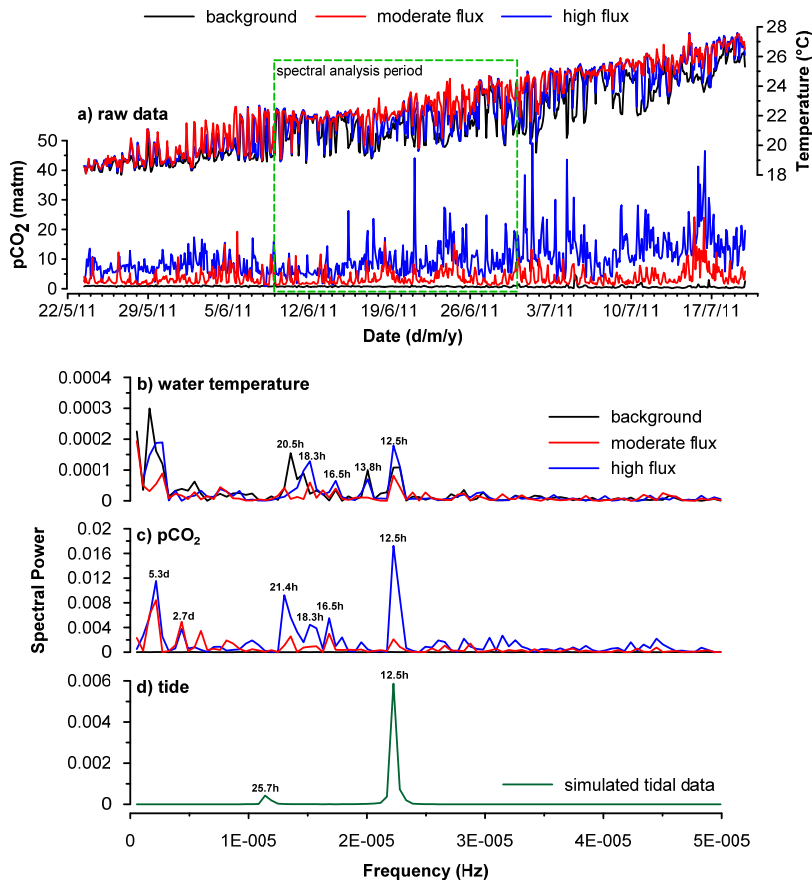


Fig. 3. (a) temperature and pCO<sub>2</sub> time series data from the first deployment, showing results from one probe per each of the three sites. Spectral analysis results of water temperature (b), pCO<sub>2</sub> (c), and simulated tidal (d) data over the period outlined in (a).

Temperature increased gradually over the deployment period (Fig. 3a), but with clear temperature excursions and oscillations that were as much as 4°C over 6 hours. A close examination of individual peaks and valleys shows that some of these events occur at all three sites (i.e. large-scale mixing of much of the water column) while others show the coldest temperatures at the deepest site and warmest at the shallowest (indicating temperature stratification).

The pCO<sub>2</sub> results also show wide variations, both for an individual probe and between the probes at the different sites (Fig. 3a). As expected, the background (BG) site yielded the lowest, most stable results, the moderate flux (MF) site gave intermediate, variable values, and the high flux (HF) site the highest, most variable data. The BG site, which occurs within an extensive *Posidonia* meadow, shows only a few minor pCO<sub>2</sub> anomalies at this scale (e.g. at 5/7/11) and thus is not strongly influenced by the relatively close proximity of the HF site (<50 m). The pCO<sub>2</sub> values at the MF site often have low values that are only slightly higher than the average value at the BG site, but with spikes that range between 5 to 20 matm. In contrast the HF site, which is located in the middle of the diffuse degassing area of Fig. 2a, shows baseline values that rarely fall below about 8 matm and spikes that reach up to 40 matm. Despite the different baseline values and scale of maximum peaks, some general trends as well as numerous specific events are common to both MF and HF probes. For example there is a general rise in pCO<sub>2</sub> values for both probes around 24/6/11 and 16/7/11, indicating large scale events affecting these two areas. A detailed comparison of individual events (not shown) highlights the common association of pCO<sub>2</sub> peaks with drops in water temperature.

The potential links between the measured pCO<sub>2</sub> and temperature values were studied by using spectral analysis on a portion of the data (dashed box, Fig. 3a). The temporal data was first transformed in the frequency domain by

performing a Fast Fourier Transform (FFT), and these results were used to calculate the power in each frequency band and generate the related power spectra. In addition to the power spectra for water temperature (Fig. 3b) and  $p\text{CO}_2$  (Fig. 3c) for all three sites, tidal data simulated for the Panarea area is also given (Fig. 3d), as none of these probes were equipped with pressure sensors. Note that while temperature spectral peaks are of a similar size at all three sites,  $p\text{CO}_2$  trends at the BG site are essentially flat. The clearest association between all three parameters occurs at 12.5 hours in correspondence with the tidal periodicity, implying that tidal currents may play a significant role in transport and mixing at this site. A direct comparison of the collected raw data and the simulated tidal trends shows an association between  $p\text{CO}_2$  peaks with low temperature events, however these events appear to occur during different segments of the tidal cycle. The next strongest correlation occurs at 16.5 hours, while other associations around 18.3 and 21 hours are less consistent. Low frequency peaks around 2.7 and 5.3 days are also observed for the  $p\text{CO}_2$  data, but are much less well defined for the temperature results.

This point monitoring of three separate sites raises many questions. For example, while deployment was expected to yield anomalies associated with that particular leakage point, why do many peak  $p\text{CO}_2$  values occur at both the HF and MF sites, located 50 m apart? If the  $\text{CO}_2$  peaks are caused by local leaks during low current conditions, why are they typically associated with lower water temperatures? What exactly is the association with the tide, as the lack of tidal currents could induce accumulation whereas the occurrence of such currents could either promote dilution with low  $\text{CO}_2$  waters or they could transport dissolved  $\text{CO}_2$  from other locations. As all probes were deployed on the seafloor, what are the trends and relationships with concentrations in the overlying water column? Spatial data is needed to address such questions, and thus the second deployment was undertaken just outside the pockmark of the HF site using multiple probes positioned along a water column transect.

### 3.2. Deployment 2

The complete dataset for all probes are given in Fig. 4, including time series data (a-c) and 2D contoured data across the transect for specific events (d-f). Note that although an Acoustic Doppler Current Profiler (ADCP) was used during this deployment, unfortunately it did not produce useable data.

The pressure data defines the tides, onto which is superimposed noise caused by waves (Fig. 4a). With the lack of current data this qualitative wave data can give some limited indications regarding wave induced mixing of the water column. These results show relatively calm seas for the first 1.5 days, rough seas for the following 1.5-2 days, followed by about 2 days of progressively calmer conditions. During the period prior to the storm the water temperatures of the various probes (Fig. 4b) show both a wide temporal variability as well as significant differences between them (indicating temporally variable stratification), while the  $p\text{CO}_2$  values (Fig. 4c) show rapid changes in concentrations with peak values from 2 to 40 matm. In correspondence with the arrival of the storm the water column becomes well mixed, as all probes give the same temperature and there is a rapid drop to background  $p\text{CO}_2$  values at all probe locations irrespective of depth. For the remainder of the monitoring period, both during and after the storm, temperature values oscillate over about  $1^\circ\text{C}$ , with alternating periods when all probes read the same value and when they show slight variations (but no strong stratification as observed before the storm). The periods with uniform temperatures tend to occur during temperature minimums while the slight variations occur during slight increases. During this same period the  $p\text{CO}_2$  values also alternate between intervals when all probes yield low baseline values and when small anomalous peaks occur in some or all of the probes (typically between 1-2 matm). Although not exact, the low uniform  $p\text{CO}_2$  periods tend to occur during periods of uniform temperatures, implying efficient mixing of the water column and active dilution.

The data from all 19 probes were contoured for each 10 minute analysis event to produce a two dimensional representation (cross-section) of the water column  $p\text{CO}_2$  and temperature distribution at that moment. All 726 sections were then merged in a single video file, which animates the 2D temporal evolution; although this is not available with this article, a video from a similar experiment conducted in 2013 is available in [5]. Instead, three representative events have been included in Fig. 4. Strong basal  $p\text{CO}_2$  anomalies are associated with the onset of clear horizontal temperature stratification (Fig. 4d) caused not by surface water warming but by the lateral ingress of cold waters along the seafloor. The co-arrival of low temperatures and high  $p\text{CO}_2$  values, which is well illustrated in the video, implies the inflow of deeper,  $\text{CO}_2$ -charged waters, possibly via upwelling currents. The resultant thermocline appears to inhibit vertical mixing of the dissolved  $\text{CO}_2$  with the overlying water column. As this

stratification becomes less marked, however, there is the potential that such anomalies can ascend (Fig. 4e), thus facilitating the eventual transfer of leaking CO<sub>2</sub> to the atmosphere. The third example shows the arrival of a pCO<sub>2</sub> anomaly not along the seafloor but rather along the entire water column on the right hand side (Fig. 4f). In contrast to the previous two sections, which were taken before the storm, this final example shows a well-mixed water column with a homogeneous temperature of about 19.9°C. It appears that this pCO<sub>2</sub> anomaly is the result of vertical mixing that, on the other hand, is laterally contained enough to maintain elevated values (about 3 matm).

Despite the unfortunate lack of current data, the reported 2D monitoring has yielded information which addresses some of the questions outlined above. The association of colder waters and high pCO<sub>2</sub> values observed during the first deployment appears to be due to the ingress of basal currents, restricted to the interval above the seafloor by temperature stratification and, likely, density increases due to the dissolved CO<sub>2</sub> itself. This would also explain the occurrence of such anomalies at the MF and HF leakage areas, as this is a more regional process not associated with the local leaks. The behavior of the measured parameters are different before and after the storm, with periods of strong stratification and high basal pCO<sub>2</sub> values characterizing the former while the lower pCO<sub>2</sub> anomalies during the latter often occur higher up in the water column during periods of small, spatially-restricted temperature anomalies. These storm and post-storm anomalies may be due to local leaks or to lateral movement from leakage areas in shallower waters near Bottaro Island.

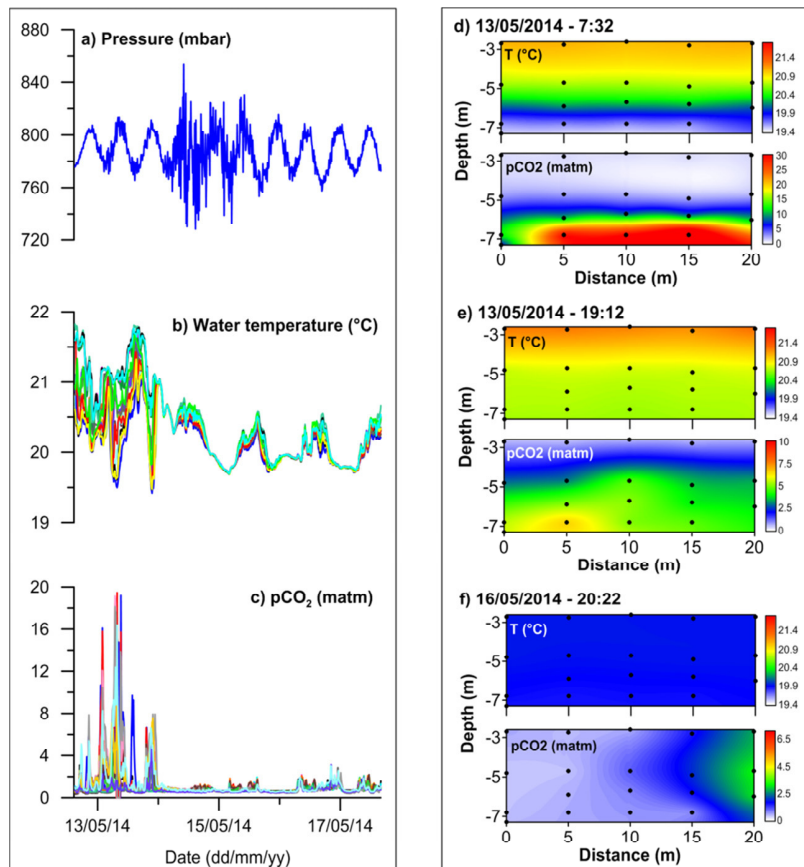


Fig. 4. Deployment 2 data from all 19 GasPro probes for pressure (a), temperature (b), and pCO<sub>2</sub> (c); because results are used to show overall trends, probe names/locations are not given; note that the Y axis for (c) is truncated from an original maximum of 40 matm to highlight the smaller peaks in the latter two-thirds of the monitored period. Contoured data along the transect from three events discussed in the text (d, e, f); while the temperature scale is the same for all three plots, the pCO<sub>2</sub> scale is different for each to highlight the observed anomalies.

### 3.3. Deployment 3

The results from four representative events during deployment 3 monitoring (Fig. 1b) are given in Fig. 5, with the colored contours showing  $p\text{CO}_2$  spatial distributions in the water column in and around a single bubble flare and the contour lines giving the water temperature distribution. Like that described for deployment 2, the 380 “snap-shots” at 10 minute intervals have been animated together in a video to show the spatial-temporal evolution. Again an ADCP was deployed but no useable data was obtained due, possibly, to interference from the bubbles.

One of the most common distributions is that illustrated in Fig. 5a, where high  $p\text{CO}_2$  values occur in the top 2 to 3 probes along the bubble flare (around 5 matm) but with significantly lower values laterally and in the lowest probe at the bubble release point (around 1 matm). The lower value at the base of the flare is likely due to lateral ingress of upwelling bottom waters caused by bubble turbulence, as shown by the central doming of the temperature contours. Such upwelling is well known and has been observed in the field, such as in studies of lacustrine diffuser systems used to combat hypoxia [6]. Upwelling results in rising bubbles being in contact with entrained water that has already dissolved  $\text{CO}_2$  into it, thus influencing the mass transfer rate between the bubble and water, and the eventual life-time of the bubbles. The dissolved  $\text{CO}_2$  flare is observed to move on the transect plane as a function of currents. A good example is given in Fig. 5b, where the lateral entrance of very slightly colder water from the left at a depth of about 15 m (causing a minor and short-lived temperature inversion) appears to shift the  $p\text{CO}_2$  flare to the right.

While entrainment involves the uplift of deeper waters with the rising bubbles, detrainment is the vertical drop-back of this water due to increased density (due to  $\text{CO}_2$  dissolution) and decreased bubble driving force higher in the water column. Although not definitive, the results in Fig. 5 c,d may show this effect at different levels within the water column. While both sections show temperature upwelling and the dissolved flare in association with the bubble plume, Fig. 5c shows anomalous values in the probes at 2.5 m above the seafloor, whereas Fig. 5d shows a similar feature at 4.5 m above the seafloor. Interpretation of these results are complicated by the occurrence of other, even stronger leakage points located about 30 to 50 m away from the transect site, and thus these high  $p\text{CO}_2$  layers may instead be due to lateral migration of a vertically restricted plume from these other sources.

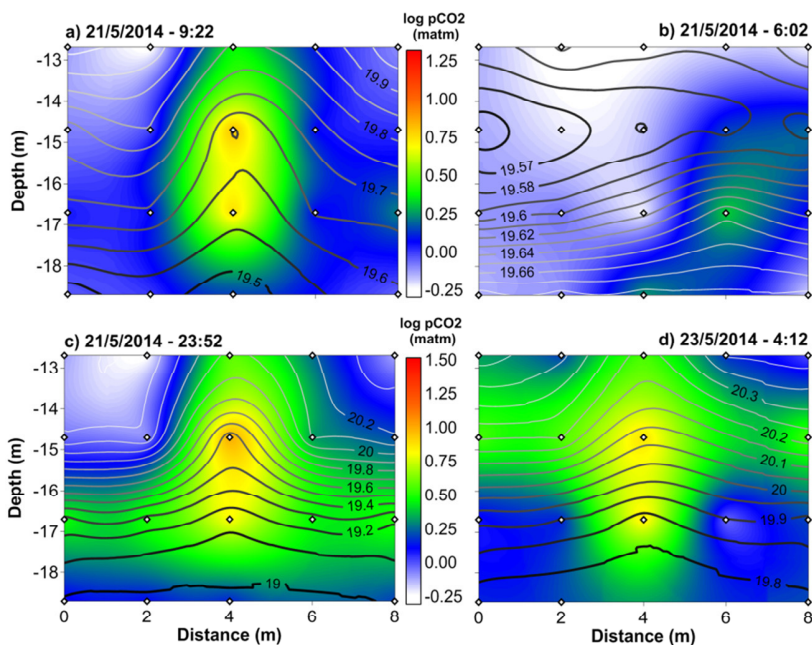


Fig. 5. Deployment 3 data contoured for four events discussed in the text (a-d). Contour lines refer to temperature in degrees Celsius (thicker, blacker lines are colder than thinner, whiter lines) while colored contours refer to  $\log p\text{CO}_2$  data in matm (note that the color scale for the upper two plots is slightly different from that for the lower two plots).

The detailed spatial-temporal monitoring of this single bubble flare has shown how concentrations in the near field reduce rapidly due to dilution moving away from the core, where the highest values are typically concentrated in the interval between 2 – 4 m above the seafloor. This reflects the rapid dissolution of CO<sub>2</sub>, combined with the complex interplay of entrainment, detrainment, and currents on mass transfer rates from the gaseous to dissolved phase and the subsequent migration of dissolved CO<sub>2</sub> within the water column. It should be noted, however, that although CO<sub>2</sub> dissolution is rapid these bubble flares tend to reach the water surface, likely due to stripping of O<sub>2</sub> and N<sub>2</sub> from the water column into bubbles that no longer hold significant quantities of CO<sub>2</sub>. It is also interesting to note that during the entire deployment there are few periods where significant anomalies occur at the seafloor, in contrast to that observed near the pockmark site during deployment 2.

#### 4. Conclusions

These experiments highlight the potential of the GasPro-pCO<sub>2</sub> sensor for a number of offshore CCS applications, including defining baseline variability, providing data for physical modelling of dissolved CO<sub>2</sub> plume dispersion, and for eventual CCS injection monitoring. The low cost and small size of each unit allows for the deployment of a large number of units and, thus, an increase in spatial resolution of temporal data. This could involve either detailed work to better understand physical-chemical processes, or for the monitoring of large areas above injection sites.

The spatial-temporal monitoring at the Panarea site has highlighted the extreme variability in pCO<sub>2</sub> values and distributions in the natural environment, an observation that is critical for both the design of site monitoring programs and for potential ecosystem impacts from a hypothetical leak. Regarding the former, the second deployment showed how monitoring near the seafloor may increase the chances of observing a leakage anomaly, as density and stratification effects combined with the rapid dissolution of CO<sub>2</sub> in the first few meters after release from the sediments may concentrate high values in that interval. That said, the third deployment only periodically showed very high values at the seafloor, indicating that site conditions must be well understood when designing a monitoring program. In particular, a clear understanding of currents prior to injection is needed to focus eventual leakage monitoring in areas that are most likely to capture anomalies, with the results presented here showing a strong link between observed results and tidal periodicity and the potential impact of storm events on transport and mixing processes. Regarding the latter, the rapidly changing pCO<sub>2</sub> values measured during all three deployments shows how impact studies on marine organisms must attempt to mimic this complex variability, as organisms be exposed to a wide range of different pCO<sub>2</sub> values over variable time periods in the near-field around a leak.

#### Acknowledgements

The authors would like to thank research colleagues Cinzia De Vittor and Cinzia Comici of OGS (Trieste, Italy) and Andrea Fogliuzzi of Amphibia Diving (Salina, Italy) for their invaluable help during the experiments. The research leading to these results has received funding from the European Union 7<sup>th</sup> Framework Programme within the ECO<sub>2</sub> project (grant agreement n° 265847) and the RISCs project (grant agreement n° 240837); the RISCs project was also funded in part by industry partners ENEL I&I, Statoil, Vattenfall AB, E.ON and RWE.

#### References

- [1] Wang ZA, Chu SN, Hoering KA. High-frequency spectrophotometric measurements of total dissolved inorganic carbon in seawater. *Environ Sci Technol* 2013; 47 (14):7840-7847; doi:10.1021/es400567k.
- [2] Merlivat L, Brault P. CARIOCA Buoy: Carbon Dioxide Monitor. *Sea Technol* 1995; 10:23-30.
- [3] Fietzek P, Fiedler B, Steinhoff T, Körtzinger A. In situ quality assessment of a novel underwater pCO<sub>2</sub> sensor based on membrane equilibration and NDIR spectrometry. *J Atmos Ocean Tech* 2014; 31:181–196; doi:10.1175/JTECH-D-13-00083.1.
- [4] Annunziatellis A, Beaubien SE, Ciotoli G, Finoina MG, Graziani S, Lombardi S. Development of an innovative marine monitoring system for CO<sub>2</sub> leaks: system design and testing. *Energy Procedia* 2009; 1(1):2333-2340; doi:10.1016/j.egypro.2009.01.303.
- [5] Graziani S, Beaubien SE, Bigi S, Lombardi S. Spatial and Temporal pCO<sub>2</sub> marine monitoring near Panarea Island (Italy) using multiple low-cost GasPro sensors. *Environ Sci Technol* 2014; 48:12126-12133; doi:10.1021/es500666u.
- [6] McGinnis DF, Lorke A, Wüest A, Stöckli A, Little JC. Interaction between a bubble plume and the near field in a stratified lake. *Water Resour Res* 2004; 40:W10206; doi:10.1029/2004WR003038.